

## Status of Dark Photons

James M. Cline

*CERN, Theoretical Physics Department, Geneva, Switzerland, and Department of Physics,  
McGill University, 3600 rue University, Montréal, Québec, Canada H3A2T8*



I review recent developments in the field of dark photons—here taken to be U(1) gauge bosons with mass less than the  $Z$ —including both kinetically mixed vectors and those that couple to anomaly-free U(1)'s. Distinctions between Higgs and Stueckelberg masses are highlighted, with discussion of swampland constraints, UV completions, and new experimental search strategies.

**1. Introduction.** As we have often been reminded, the possible range of viable dark matter (DM) masses spans many orders of magnitude, and this is also true for DM in the form of U(1) vector gauge bosons. The heavier version is usually called a  $Z'$  in the literature, whereas lighter ones are called dark photons. I take the the  $Z^0$  mass to be the upper boundary in this review of dark photons, while below the lower limit  $\sim 10^{-22}$  eV, such particles would have too long a de Broglie wavelength to function as dark matter in galaxies.<sup>1</sup> Below this limit, dark photons could still play an interesting role in a larger dark sector, such as binding dark atoms and giving rise to millicharged dark matter (see Ref.<sup>2</sup> for a review). Here I will not discuss massless dark photons except as an approximation to massive ones in the case where the masses are negligible relative to relevant energy scales.

Hence, the dark photon could play the role of dark matter, dark force mediator, or possibly both. There are two ways in which it could interact with the standard model: through kinetic mixing, which is generically expected to be present, or by coupling to an anomaly-free U(1) such  $B - L$  or a difference between two lepton flavors.

We first recall how kinetic mixing works.<sup>3</sup> The Lagrangian for the SM U(1) gauge boson (either hypercharge, above the electroweak symmetry breaking scale, or electromagnetism below it) plus the dark one is

$$\mathcal{L} = -\frac{1}{4}F_{\mu\nu}F^{\mu\nu} - \frac{1}{4}F'_{\mu\nu}F'^{\mu\nu} - \frac{1}{2}\epsilon F_{\mu\nu}F'^{\mu\nu} - \frac{1}{2}m_{A'}^2 A'_\mu A'^\mu. \quad (1)$$

If  $m_{A'}$  is nonzero, the kinetic term is diagonalized (up to  $O(\epsilon^2)$  corrections) by  $A_\mu \rightarrow A_\mu - \epsilon A'_\mu$ . Then the dark photon will couple to particles of charge  $qe$  in the SM with strength  $\epsilon qe$ .<sup>a</sup> It is

<sup>a</sup> If  $m_{A'} = 0$ , one can instead diagonalize the kinetic term using  $A'_\mu \rightarrow A'_\mu + \epsilon A_\mu$ . In this case, dark sector

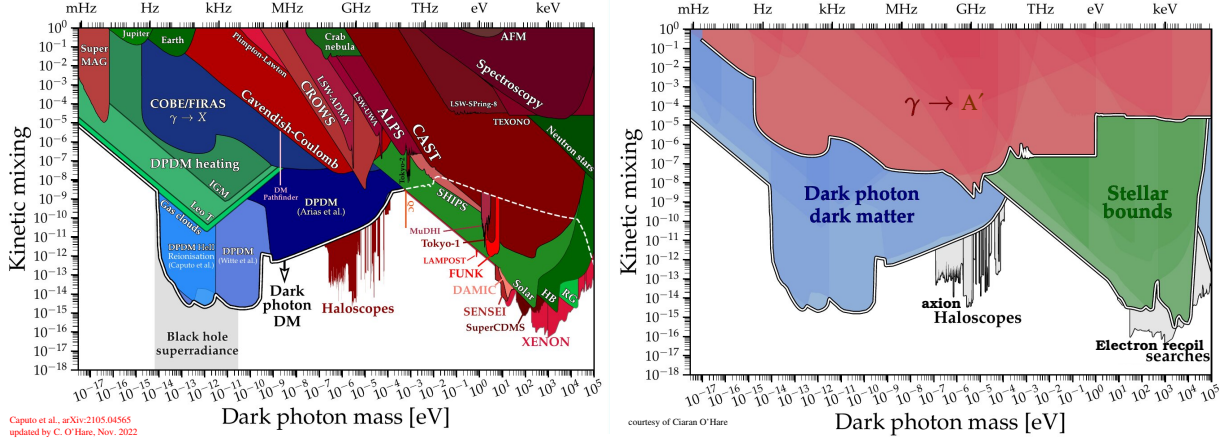


Figure 1 – Left: recent limits on kinetic mixing versus mass, from Ref. <sup>7</sup>, with updates from C. O’Hare. Right: how the constraints are grouped by categories. Figure courtesy of C. O’Hare.

interesting to notice that citations of Holdom’s seminal paper started to rise steeply in 2008, after the appearance of Refs. <sup>4,5</sup>, that highlighted the importance of kinetic mixing in extended dark sectors.

**2. Constraints on kinetic mixing.** Experimental constraints on  $\epsilon$  versus  $m_{A'}$  have evolved dramatically since 2008, when there were just a handful of limits <sup>16</sup>. Fig. 1 shows the current bounds individually (left) and as classes (right). The red region overlaps with laboratory limits:  $1/r^2$  force law tests, light-shining-through-walls, helioscopes, axion haloscopes, dark matter direct detectors, and a reactor neutrino experiment. The strongest current limit  $\epsilon \lesssim 10^{-16}$  at  $m_{A'} \sim \text{keV}$  comes from  $A'$  absorption by atoms in the XENON1T experiment.<sup>8</sup>

The red region also includes constraints from SM photons resonantly converting to  $A'$ , due to the photon plasma mass matching  $m_{A'}$  in the cosmic microwave background, which would distort the cosmic microwave background, CMB (COBE/FIRAS constraint). The green region arises from  $\gamma \rightarrow A'$  in stars, which would cause the stars to cool faster than observed. The foregoing constraints exist independently of whether  $A'$  is the DM. If it is the DM, then the blue regions are constrained by  $A' \rightarrow \gamma$  causing reionization of helium in interstellar gas clouds.<sup>7</sup>

Axion haloscopes are an example of experiments designed for different physics whose limits can be reinterpreted in terms of dark photon detection.<sup>9,10</sup> When the cavity frequency matches  $m_{A'}$ , there are resonant photon- $A'$  oscillations, without the need for an external magnetic field. Recently it was shown that radio telescopes can be sensitive to conversion of  $A' \rightarrow \gamma$  in the dish leading to a monochromatic signal. Assuming  $A'$  is the DM, LOFAR data rule out  $\epsilon \gtrsim 10^{-13}$  for  $m_{A'} \sim 10^{-7} \text{ eV}$ ,<sup>11</sup> and FAST excludes  $\epsilon \gtrsim 10^{-12}$  for  $m_{A'} \sim 10^{-5} \text{ eV}$ .<sup>12</sup> These limits are projected to improve, especially with future SKA data. A conceptually similar constraint is shown to arise in the optical from the James Webb Space Telescope,<sup>13</sup> leading to  $\epsilon \lesssim 10^{-11}$  for  $m_{A'} \sim (0.05 - 2) \text{ eV}$ .

So far we discussed light dark photons,  $m_{A'} < \text{MeV}$ . Different kinds of constraints apply for heavier  $A'$ , notably from an array of beam-dump and collider experiments. Fig. 2 (top row) illustrates these limits in the case where  $A'$  couples to DM  $\chi$  of mass  $m_\chi = m_{A'}/4$  and coupling  $g_\chi = 0.1$  or  $1$ . The laboratory constraints depend on  $g_\chi$  because it increases the invisible width of  $A'$ . However they generally resemble those arising from purely visible decays of  $A'$ . (The cyan regions are disfavored by assuming freeze-in of DM through its interactions with  $A'$ .)

Model-dependent bounds have been obtained at LHC, illustrated in Fig. 2 (bottom left). If the SM Higgs has a significant branching ratio into dark fermions, which decay to  $A'$  plus DM, the subsequent decays of  $A' \rightarrow \mu^+ \mu^-$  yield strong limits, depending on whether they are prompt

particles coupling to  $A'$  become millicharged. In the limit of small  $m_{A'}$ , where  $A'$  can be approximated as massless, for example in a stellar environment, the dark Higgs looks millicharged, which leads to strong constraints.

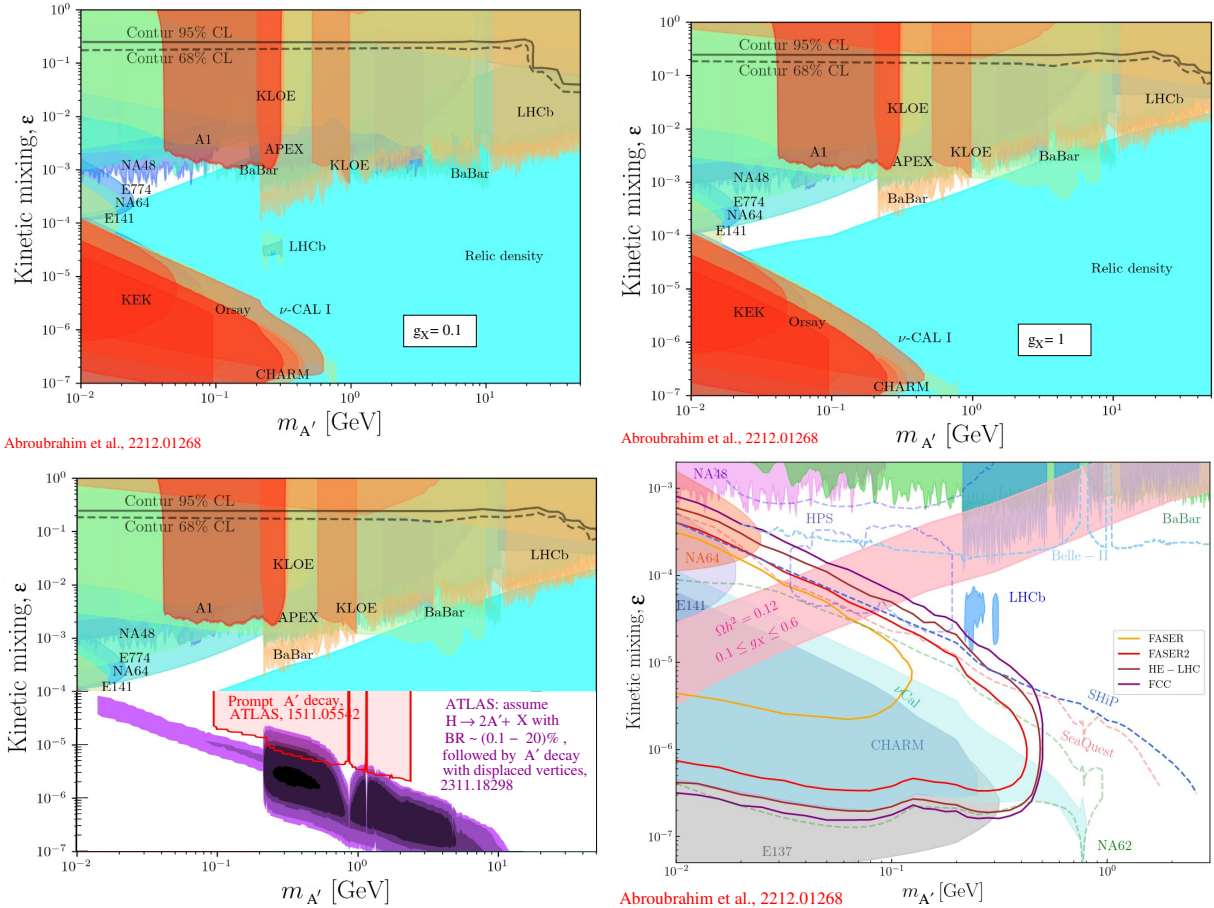


Figure 2 – Top row: laboratory limits on kinetic mixing versus mass, with  $A'$  decaying to lighter DM with coupling  $g_X = 0.1$  (left) or 1 (right), from Ref. <sup>14</sup>. Cyan region assumes DM freeze-in via kinetic mixing. Bottom row: (left) ATLAS constraints from Higgs decay to dark fermions, which then decay to  $A'$  plus DM,<sup>15</sup> (right) anticipated sensitivity of future experiments for the heavy- $A'$  parameter space.<sup>14</sup>

or displaced.<sup>15</sup> Reach of existing and proposed experiments to further probe the parameter space is shown in the bottom right panel. These include HPS, FASER, SHiP, SeaQuest, HE-LHC, and FCC.

**3. Higgs or Stueckelberg mass?** In presenting the previous bounds, it was implicitly assumed that the  $A'$  gets its mass by the Stueckelberg “mechanism,” which essentially means putting in a bare mass term as in Eq. (1) with no other degrees of freedom. One can restore gauge invariance by introducing a fictitious field  $\theta$  and rewriting the mass term as

$$\frac{1}{2}m_{A'}^2(A'^\mu - \partial^\mu\theta)^2, \quad (2)$$

but this by itself has no additional physical significance. On the other hand, if  $A'$  gets its mass from a dark scalar  $h'$  by the Higgs mechanism, one might expect  $m_{h'} \sim m_{A'}$ . If this is the case, then  $h'$  behaves like a light millicharged particle, if  $m_{A'}$  is small compared to the energy scale of interest. There is a vertex  $g'm_{A'}h'A'^2$  which leads to  $2\epsilon g'm_{A'}A'^\mu A_\mu$  in conjunction with kinetic mixing. This yields much stronger constraints on  $\epsilon$ , ruling out large regions that were allowed for the Stueckelberg case, as shown in Fig. 3. For example, stellar cooling is accelerated by Bremsstrahlung of  $h'$  from photons.<sup>16</sup> Further limits arise from production of  $h'$  in DM direct detection experiments through ionization of atoms in the detector by  $A'$  produced in the sun.<sup>17</sup> These limits however are model-dependent, because of the assumption  $m_{h'} \sim m_{A'}$  and  $g' \sim e$ .

Typically, phenomenological studies assume that there is no analog of the Higgs field corresponding to the Stueckelberg mechanism, but in consistent UV completions, namely string theory, the field  $\theta$  in (2) can be thought of as an axion-like degree of freedom, that has an

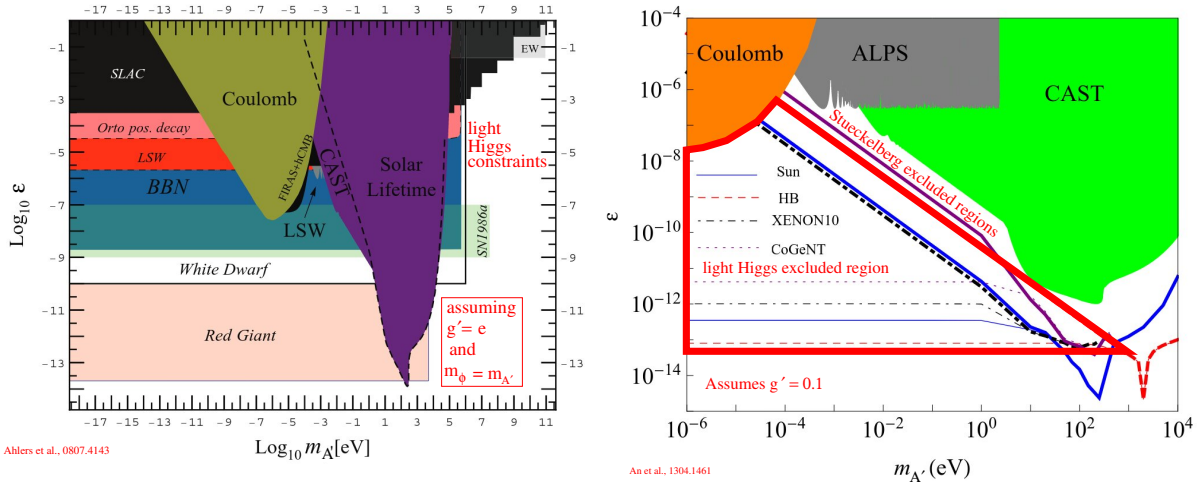


Figure 3 – Left: enlarged exclusion regions for a light dark Higgs from stellar cooling, SN1987a, and other effects.<sup>16</sup> Right: similar constraints, also including  $h'$  production in DM detection experiments.<sup>17</sup>

accompanying radial excitation  $\phi$ . Unlike the Higgs mechanism, the  $A'$  mass arises without  $\phi$  getting a VEV, and the limit  $\phi \rightarrow 0$  in field space is singular because of a kinetic term of the form  $(\partial \ln \phi)^2$ .<sup>18</sup> In contrast to Higgs masses, the limit  $m_{A'} \rightarrow 0$  is thus inconsistent in the Stueckelberg case.

Light Stueckelberg masses can naturally arise in large volume string compactifications, but there is a lower limit on the mass, which is related to the dimensionless volume  $\mathcal{V}$  of the compactification and thereby the string scale  $m_s$  and the Planck mass, through  $m_P^2 = (4\pi/g_s^2)\mathcal{V}m_s^2$ . The  $A'$  mass is of order<sup>19</sup>  $m_{A'} \sim g_s^{3/2}(m_P/\mathcal{V}) \gtrsim g_s^{3/2} \text{ eV} \gtrsim 1 \text{ eV}$ , using  $m_s \gtrsim 1 \text{ TeV}$  (from collider limits), hence  $\mathcal{V} \lesssim 10^{27}$ .

**4. Origin of kinetic mixing.** The kinetic mixing operator  $F_{\mu\nu}F'^{\mu\nu}$  has dimension 4, so its coefficient  $\epsilon$  can be put in “by hand.” But usually one imagines that it gets generated at some high scale by integrating out a heavy particle that carries both  $U(1)'$  and SM  $U(1)$  charges. In that case, its natural value is of order  $eg'/(16\pi^2)$ . To reconcile this with the XENON1T limit would require  $g' < 10^{-11}$ , precluding gauge unification. Otherwise, one could forbid matter charged under both gauge groups, but this violates a strong version of the weak gravity conjecture<sup>21</sup> (WGC, see below), which is supported by known string compactifications.

If one ignores WGC and assumes  $\epsilon = 0$  the Planck scale, then pure gravity plus Higgs mediation can generate  $\epsilon$  through a 6-loop diagram, involving three graviton exchanges and one Higgs from each (SM and dark) sector.<sup>20</sup> It is also possible to evade the WGC constraints by having exchanges of several heavy states in the loops whose contributions cancel each other. This can happen naturally in string theory compactifications,<sup>22,23</sup> where the interaction that generates the kinetic mixing is a closed string exchange between two  $D$ -branes, which host the respective  $U(1)$  matter fields (Fig. 4). Small kinetic mixing can arise from large-volume compactifications with  $\mathcal{V} = (2\pi R)^6$  (in string length units  $\ell_s = 2\pi\sqrt{\alpha'}$ ), which are associated with a light volume modulus of mass<sup>24</sup>  $m_{\mathcal{V}} \sim m_P\mathcal{V}^{-3/2}$ . The kinetic mixing is related to  $m_{\mathcal{V}}$  by<sup>23,19</sup>  $\epsilon \gtrsim 10^{-16} (m_{\mathcal{V}}/2m_h)^{8/9}$ , where  $m_h$  is the SM Higgs mass. To avoid overclosure of the Universe by such moduli, they must be heavy enough to decay into two Higgs bosons, hence this gives a lower bound on  $\epsilon$  that is close to the XENON1T constraint.

**5. DM Relic density from dark photons.** In contrast to axions or other light spin-0 DM candidates, the misalignment mechanism (where the field is stuck at a nontrivial value while the Hubble rate  $H$  exceeds its mass, and starts oscillating in its potential subsequently) does not easily account for a significant dark photon relic density. This is because vector fields in a nontrivial gravitational background couple to the Ricci scalar in such a way as to be diluted by the expansion of the Universe. One needs to introduce a nonminimal coupling  $RA'_\mu A'^\mu$  to

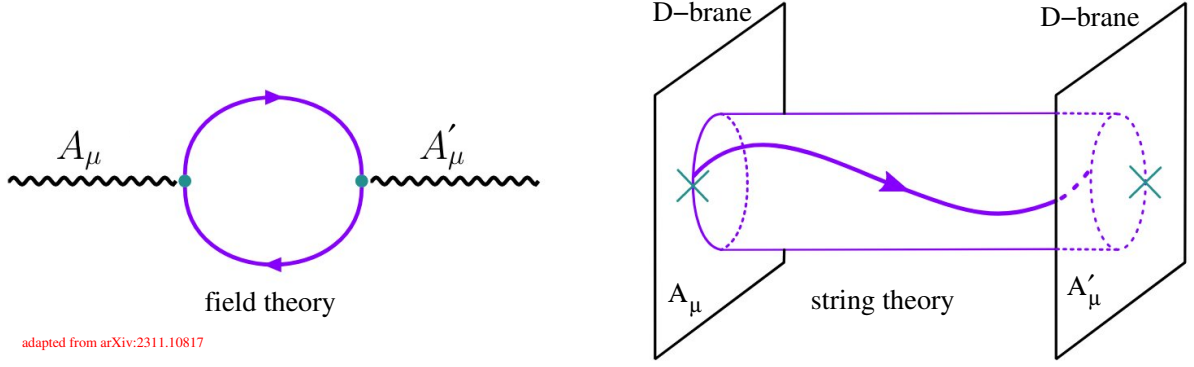


Figure 4 – String theoretic origin of kinetic mixing between two U(1)’s localized on different  $D$  branes (right) versus field theory diagram (left), from Ref. <sup>23</sup>.

counteract this effect,<sup>9,25</sup> but doing so leads to the longitudinal polarization becoming ghost-like for some range of momenta.<sup>26</sup> This can be overcome by modifying the kinetic term by coupling it to a scalar field (the inflaton) via  $f(\phi)F'_{\mu\nu}F'^{\mu\nu}$ ,<sup>27</sup> but this involves significantly more model building than for a spin-0 particle, which only needs a quadratic potential for misalignment to work.

Alternatively, a generic mechanism is through inflationary fluctuations of  $A'$ , which like for any approximately massless field are of order  $H_I$ , the Hubble rate during inflation. Ref. <sup>28</sup> showed that the desired relic density is achieved if  $m_{A'} \cong 6 \times 10^{-6} \text{ eV} (10^{14} \text{ GeV}/H_I)^4$ . Another relatively simple mechanism is to couple dark photons to an axion via  $-(\beta/f_a)aF'^{\mu\nu}\tilde{F}'^{\mu\nu}$ .<sup>29,30</sup> The axion can be produced by misalignment; when it starts to oscillate, a tachyonic instability quickly transfers energy from  $a$  to  $A'_\mu$  over a wide range of axion masses and  $A'$  masses, spanning  $m_{A'} \sim (10^{-7} - 10^7) \text{ eV}$ . A similar mechanism works for dark Higgs oscillations producing  $A'$  pairs by parametric resonance.<sup>31</sup>

Dark photons can also serve as the mediator that gives rise to thermal relic dark matter through the classic processes  $\chi\bar{\chi} \rightarrow A'A'$  or  $\chi\bar{\chi} \rightarrow A'^* \rightarrow f\bar{f}$ . However there are many other possible production pathways that were explored in Ref. <sup>32</sup>. For example, kinetic mixing can be enhanced through resonant  $A \rightarrow A'$  conversion at finite temperature, when  $m_{A'}$  coincides with the photon plasmon mass.

**6. Swampland constraints.** The weak gravity conjecture has strong evidence, and its variants are well motivated by string theory/quantum gravity arguments. The magnetic WGC implies a UV cutoff  $\Lambda > \sqrt{m_P m_{A'}/g'}$  for Stueckelberg masses.<sup>18</sup> Since  $\Lambda > H_I$  during inflation for a consistent description, the inflationary production mechanism for  $A'$  becomes limited to masses  $m_{A'} \gtrsim 0.3 \text{ eV}$ , a very significant restriction. The WGC also demands that  $\Lambda < g'm_P$ , which combined with the generic loop estimate for  $\epsilon$  implies that  $\Lambda \lesssim (16\pi^2/e)\epsilon m_P \sim 100 \text{ TeV}$  (using the XENON constraint on  $\epsilon$ ),<sup>33</sup> suggesting new states would be accessible at the Future Circular Collider. Similarly, combining the magnetic WGC with the LHC bound  $\Lambda \gtrsim 10 \text{ TeV}$  and the loop estimate for  $\epsilon$  disfavors a large region of parameter space,<sup>34</sup> including interesting values  $m_{A'} \sim 10^{-11}$ ,  $\epsilon \sim 10^{-7}$  where axion decays  $a \rightarrow A'A'$  followed by  $A' \rightarrow A$  resonant oscillations can boost the spectrum of low-frequency CMB photons, suppressing the 21 cm signal as seen by the EDGES collaboration.<sup>35,36</sup>

**7. Nonabelian kinetic mixing and Composite dark photons.** It was realized early on<sup>4</sup> that the photon could kinetically mix with a nonabelian gauge boson through the diagram

$$\begin{array}{c}
 \gamma \text{ wavy line} \quad e \quad \text{circle with } X \quad \begin{array}{l} \text{g}' \\ \text{wavy line } G'_B \\ \text{y}_X \text{ dashed line } \Phi_B \end{array} \\
 \sim \frac{y_X e g' \langle \Phi \rangle}{16\pi^2 M_X}
 \end{array}$$

where  $\Phi$  gets a VEV and breaks the gauge symmetry. Then kinetic mixing comes from a

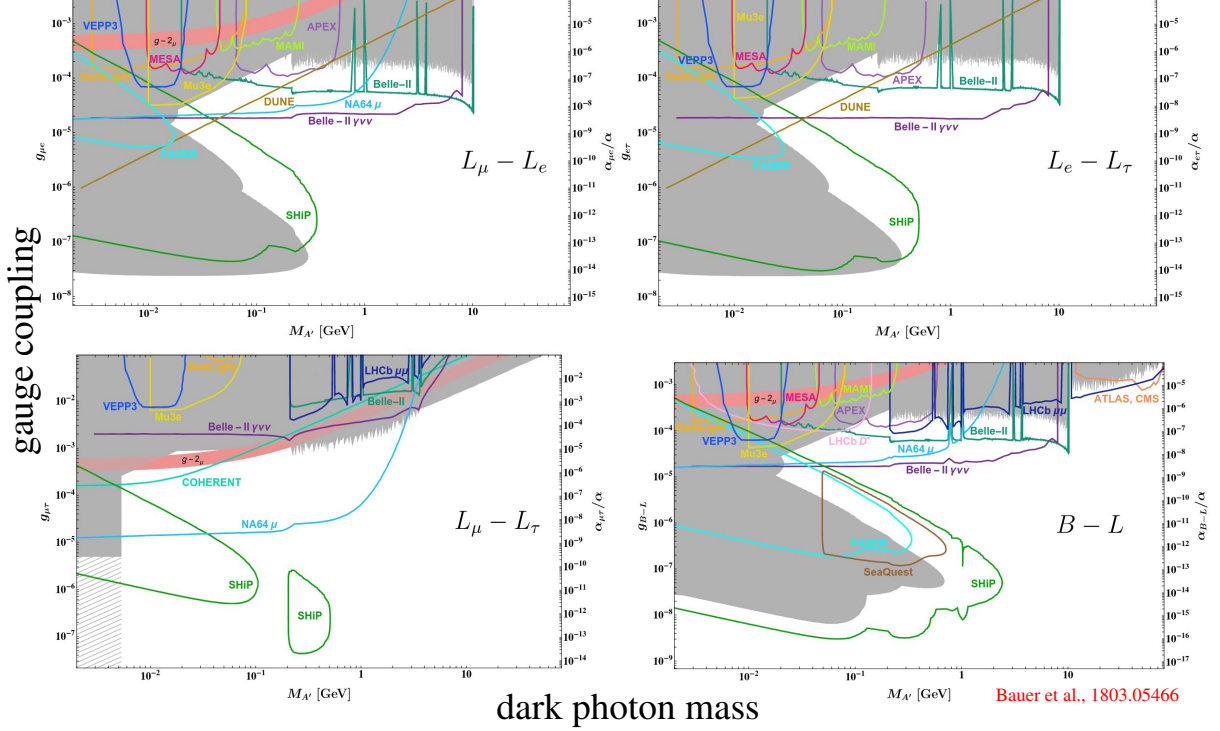


Figure 5 – Constraints on gauge coupling versus  $m_{A'}$  for the four anomaly-free gauge groups, from Ref. <sup>38</sup>.

dimension-5 operator, giving another possibility for suppressing  $\epsilon$ , without needing small  $g'$ . It was pointed out<sup>37</sup> that this can also work in a confining phase, where  $\langle \Phi \rangle = 0$ ; for example  $\Phi$  binds with the dark gluon to form a massive composite dark photon  $\tilde{A}$ , with  $\epsilon \sim \sqrt{\alpha\alpha'} y_X \Lambda / (4\pi m_X)$ , where  $\Lambda$  is the dark confinement scale. An interesting feature is that the kinetic mixing  $\epsilon$  can be correlated with  $m_{\tilde{A}} \sim \Lambda$  by their dependence on  $\Lambda$  (note that  $\alpha' \sim 1/\ln \Lambda$  is not independent). Dark baryons provide a natural DM candidate in such models, and can have direct detection signals by mediation of  $\tilde{A}$ .

**8. Gauging SM global symmetries.** In addition to kinetic mixing,  $A'$  could couple directly to SM particles by gauging one of its global symmetries. The simplest possibilities involve anomaly-free combinations,  $B - L$ ,  $L_e - L_\mu$ ,  $L_e - L_\tau$  and  $L_\mu - L_\tau$  since then no further matter content is required (except possibly right-handed neutrinos). If  $\epsilon = 0$  at a high scale, then it is calculable at lower scales.<sup>38</sup> For example  $\epsilon \sim eg' \ln(m_\tau/m_\mu)/(4\pi^2) \sim 0.036 g'$  for gauged  $L_\mu - L_\tau$  at vanishing momentum transfer  $q^2 = 0$ ; hence it makes a subdominant contribution to observable processes.

Constraints on  $g'$  versus  $m_{A'}$  for the gauged models are shown in Fig. 5. They are most severe when  $A'$  couples to electrons, making  $L_\mu - L_\tau$  a special case. In fact, it is the only one that can explain the muon  $g - 2$  anomaly (through one-loop dressing of the muon vertex by  $A'$  exchange), illustrated by the narrow pink band. For the same reason, kinetically mixed models are also ruled out for  $(g - 2)_\mu$  (see Ref. <sup>39</sup> for a loophole).

From a model-building standpoint, it might seem arbitrary to gauge only  $L_\mu - L_\tau$  as opposed to other flavor combinations, but Ref. <sup>40</sup> showed that such a vector boson could be just the lightest of eight such, coming from the gauging of SU(3) lepton flavor, broken at the (5 – 10) TeV scale, except for one scalar in the 6 representation with VEV (20 – 200) GeV to explain the lightest vector mass. The model predicts heavy neutral leptons at the GeV scale, constrained by BBN, and that the lightest neutrino has mass  $m_{\nu_1} \gtrsim 10^{-4}$  eV. It can also address the Cabbibo anomaly.

The  $L_\mu - L_\tau$  dark photon can have interesting implication for neutrino physics if it is the dark matter. One can treat it as an oscillating condensate which gives a time-dependent effective mass to  $\nu_\mu$  and  $\nu_\tau$ , with potential impact on neutrino oscillations. This can re-open parameter

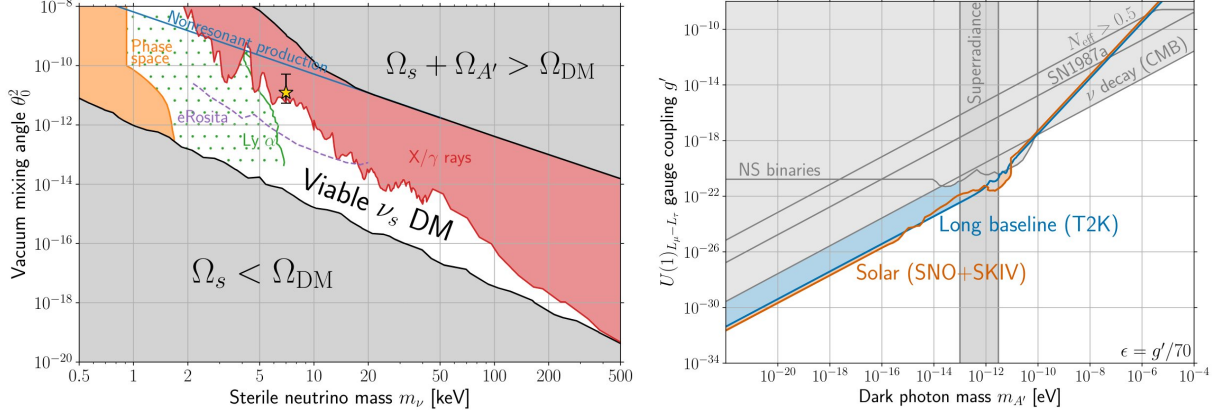


Figure 6 – Left: re-opened region of active-sterile neutrino mixing angle versus sterile  $\nu$  mass, enabled by  $L_{\mu} - L_{\tau}$  dark photon dark matter.<sup>41</sup> Right: constraints on the  $L_{\mu} - L_{\tau}$  gauge coupling versus  $m_{A'}$  from distortions of long baseline and solar neutrino oscillations by  $L_{\mu} - L_{\tau}$  dark photon DM.<sup>44</sup>

space for sterile neutrino dark matter, by making  $\nu_s - \nu_{\mu}$  oscillations resonant and thereby making  $\nu_s$  production efficient at smaller mixing angles than ordinarily required,<sup>41</sup> this is illustrated in Fig. 6 (left). Similarly, this effect can impact oscillations between active neutrino flavors,<sup>42,43,44</sup> giving rise to leading constraints on the coupling, as shown in Fig. 6 (right). It was recently shown that  $B - L$  dark photons can be probed through dark matter-neutrino scattering if the DM carries  $B - L$ , using IceCube observations of neutrinos from the active galaxy NGC 1068.<sup>45</sup> Dark matter self-interactions mediated by dark photons might also play a role in accelerating the mergers of supermassive black holes,<sup>46</sup> to overcome the long-standing “final parsec” problem.

**Acknowledgments.** This work was supported by the Natural Sciences and Engineering Research Council (NSERC) of Canada. I thank J. Jaeckel, C. O’Hare, M. Tytgat and S. Witte for helpful discussions, and the CERN theory department for its generous hospitality.

## References

1. L. Hui, J. P. Ostriker, S. Tremaine and E. Witten, Phys.Rev. D **95**, no.4, 043541 (2017) [arXiv:1610.08297 [astro-ph.CO]].
2. J. M. Cline, SciPost Phys.Lect. Notes **52**, 1 (2022) [arXiv:2108.10314 [hep-ph]].
3. B. Holdom, Phys.Lett. B **166**, 196-198 (1986)
4. N. Arkani-Hamed, D. P. Finkbeiner, T. R. Slatyer and N. Weiner, Phys.Rev. D **79**, 015014 (2009) [arXiv:0810.0713 [hep-ph]].
5. M. Pospelov, A. Ritz and M. B. Voloshin, Phys.Lett.B **662**, 53-61 (2008) [arXiv:0711.4866].
6. M. Ahlers, J. Jaeckel, J. Redondo and A. Ringwald, Phys.Rev. D **78**, 075005 (2008) [arXiv:0807.4143 [hep-ph]].
7. A. Caputo, A. J. Millar, C. A. J. O’Hare and E. Vitagliano, Phys.Rev. D **104**, no.9, 095029 (2021) [arXiv:2105.04565 [hep-ph]].
8. E. Aprile *et al.* [XENON], Phys.Rev. Lett. **123**, no.25, 251801 (2019) [arXiv:1907.11485].
9. P. Arias, D. Cadamuro, M. Goodsell, J. Jaeckel, J. Redondo and A. Ringwald, JCAP **06**, 013 (2012) [arXiv:1201.5902 [hep-ph]].
10. S. Ghosh, E. P. Ruddy, M. J. Jewell, A. F. Leder and R. H. Maruyama, Phys.Rev. D **104**, no.9, 092016 (2021) [arXiv:2104.09334 [hep-ph]].
11. H. An, X. Chen, S. Ge, J. Liu and Y. Luo, Nature Commun. **15**, no.1, 915 (2024) [arXiv:2301.03622 [hep-ph]].
12. H. An, S. Ge, W. Q. Guo, X. Huang, J. Liu and Z. Lu, Phys.Rev. Lett. **130**, no.18, 181001 (2023) [arXiv:2207.05767 [hep-ph]].
13. H. An, S. Ge, J. Liu and Z. Lu, [arXiv:2402.17140 [hep-ph]].

14. A. Aboubrahim, M. M. Altakach, M. Klasen, P. Nath and Z. Y. Wang, *JHEP* **03**, 182 (2023) [arXiv:2212.01268 [hep-ph]].
15. G. Aad *et al.* [ATLAS], [arXiv:2311.18298 [hep-ex]].
16. M. Ahlers, J. Jaeckel, J. Redondo and A. Ringwald, *Phys.Rev. D* **78**, 075005 (2008) [arXiv:0807.4143 [hep-ph]].
17. H. An, M. Pospelov and J. , *Phys.Rev. Lett.* **111**, 041302 (2013) [arXiv:1304.3461].
18. M. Reece, *JHEP* **07**, 181 (2019) [arXiv:1808.09966 [hep-th]].
19. M. Goodsell, J. Jaeckel, J. Redondo and A. Ringwald, *JHEP* **11**, 027 (2009) [arXiv:0909.0515 [hep-ph]].
20. T. Gherghetta, J. Kersten, K. Olive and M. Pospelov, *Phys.Rev. D* **100**, no.9, 095001 (2019) [arXiv:1909.00696 [hep-ph]].
21. N. Arkani-Hamed, L. Motl, A. Nicolis and C. Vafa, *JHEP* **06**, 060 (2007) [arXiv:hep-th/0601001 [hep-th]].
22. G. Obied and A. Parikh, [arXiv:2109.07913 [hep-ph]].
23. A. Hebecker, J. Jaeckel and R. Kuespert, *JHEP* **04**, 116 (2024) [arXiv:2311.10817 [hep-th]].
24. J. P. Conlon, F. Quevedo and K. Suruliz, *JHEP* **08**, 007 (2005) [arXiv:hep-th/0505076].
25. A. Golovnev, V. Mukhanov and V. Vanchurin, *JCAP* **06**, 009 (2008) [arXiv:0802.2068].
26. M. Karciauskas and D. H. Lyth, *JCAP* **11**, 023 (2010) [arXiv:1007.1426 [astro-ph.CO]].
27. K. Nakayama, *JCAP* **10**, 019 (2019) [arXiv:1907.06243 [hep-ph]].
28. P. W. Graham, J. Mardon and S. Rajendran, *Phys.Rev. D* **93**, no.10, 103520 (2016) [arXiv:1504.02102 [hep-ph]].
29. P. Agrawal, N. Kitajima, M. Reece, T. Sekiguchi and F. Takahashi, *Phys.Lett. B* **801**, 135136 (2020) [arXiv:1810.07188 [hep-ph]].
30. R. T. Co, A. Pierce, Z. Zhang and Y. Zhao, *Phys.Rev. D* **99**, no.7, 075002 (2019) [arXiv:1810.07196 [hep-ph]].
31. J. A. Dror, K. Harigaya and V. Narayan, *Phys.Rev. D* **99**, no.3, 035036 (2019) [arXiv:1810.07195 [hep-ph]].
32. T. Hambye, M. H. G. Tytgat, J. Vandecasteele and L. Vanderheyden, *Phys.Rev. D* **100**, no.9, 095018 (2019) [arXiv:1908.09864 [hep-ph]].
33. K. Benakli, C. Branchina and G. Lafforgue-Marmet, *Eur. Phys. J. C* **80**, no.12, 1118 (2020) [arXiv:2007.02655 [hep-ph]].
34. M. Montero, J. B. Muñoz and G. Obied, *JHEP* **11**, 121 (2022) [arXiv:2207.09448 [hep-ph]].
35. M. Pospelov, J. Pradler, J. T. Ruderman and A. Urbano, *Phys. Rev. Lett.* **121**, no.3, 031103 (2018) [arXiv:1803.07048 [hep-ph]].
36. A. Caputo, H. Liu, S. Mishra-Sharma, M. Pospelov, J. T. Ruderman and A. Urbano, *Phys. Rev. Lett.* **127**, no.1, 011102 (2021) [arXiv:2009.03899 [astro-ph.CO]].
37. G. Alonso-Álvarez, R. Cao, J. M. Cline, K. Moorthy and T. Xiao, *JHEP* **02**, 017 (2024) [arXiv:2309.13105 [hep-ph]].
38. M. Bauer, P. Foldenauer and J. Jaeckel, *JHEP* **07**, 094 (2018) [arXiv:1803.05466 [hep-ph]].
39. G. Mohlabeng, *Phys. Rev. D* **99**, no.11, 115001 (2019) [arXiv:1902.05075 [hep-ph]].
40. G. Alonso-Álvarez and J. M. Cline, *JHEP* **03**, 042 (2022) [arXiv:2111.04744 [hep-ph]].
41. G. Alonso-Álvarez and J. M. Cline, *JCAP* **10**, 041 (2021) [arXiv:2107.07524 [hep-ph]].
42. V. Brdar, J. Kopp, J. Liu, P. Prass and X. P. Wang, “Fuzzy dark matter and nonstandard neutrino interactions,” *Phys. Rev. D* **97**, no.4, 043001 (2018) doi:10.1103/PhysRevD.97.043001 [arXiv:1705.09455 [hep-ph]].
43. D. Brzemiński, S. Das, A. Hook and C. Ristow, *JHEP* **08**, 181 (2023) doi:10.1007/JHEP08(2023)181 [arXiv:2212.05073 [hep-ph]].
44. G. Alonso-Álvarez, K. Bleau and J. M. Cline, *Phys. Rev. D* **107**, no.5, 055045 (2023) [arXiv:2301.04152 [hep-ph]].
45. J. M. Cline and M. Puel, *JCAP* **06**, 004 (2023) [arXiv:2301.08756 [hep-ph]].
46. G. Alonso-Álvarez, J. M. Cline and C. Dewar, [arXiv:2401.14450 [astro-ph.CO]].